Trans Indian Inst Met (2020) 73(10):2587–2600
https://doi.org/10.1007/s12666-020-02075-8

ORIGINAL ARTICLE

Modeling and Optimization of the Yield Strength and Tensile Strength of Al7075 Butt Joint Produced by FSW and SFSW Using RSM and Desirability Function Method

Mahdi Vahdati[1] · **Mahmoud Moradi**[2] · **Mahmoud Shamsborhan**[3,4]

Received: 21 April 2020 / Accepted: 10 August 2020 / Published online: 19 August 2020

Abstract Friction stir welding (FSW) is introduced as a solid-state welding process. Despite the many benefits of the FSW, the effects of the thermal cycles in this process are causing softening of the joint. This phenomenon generally occurs in heat-treatable aluminum alloys and results in reduced mechanical properties of the joint. To solve this limitation, submerged friction stir welding (SFSW) has been developed which is suitable for welding of heat-sensitive alloys. In this study, 31 butt joints were first produced from Al7075-T6 using the FSW. For this purpose, the response surface methodology was selected as the design of experiments method, and the variables: tool rotational speed, tool feed rate, tool shoulder diameter, and tool tilt angle were determined as the input variables. Then, the statistical analysis of the parameters affecting the yield strength and tensile strength of the joints was investigated. Then, 10 joints were produced using the SFSW based on the optimal values of the tool feed rate and tool tilt angle. Results of the ANOVA and regression analysis of the experimental data confirmed the accuracy and precision of regression equations and showed that the linear, interactional and quadratic terms of tool shoulder diameter and tool rotational speed effect on the yield strength and ultimate tensile strength of submerged joints. Also, the optimal conditions of input variables were determined by the desirability method and confirmed by the verification test.

Keywords Modeling · Optimization · Yield strength · Tensile strength · Friction stir welding · Response surface methodology

1 Introduction

Joining of magnesium [1] and aluminum [2] alloys with fusion welding processes has always had a variety of problems. Defects such as crack, void, and porosity affect the quality and mechanical properties of the weld during fusion welding. A solid-state welding process known as friction stir welding (FSW) was developed by the welding institute (TWI) [3] in the 1990s. This process is suitable for the welding of materials that are difficult with fusion welding processes. In this process, the temperature remains below the solidus temperature, and no melting occurs. Therefore, common defects of the fusion welding do not appear in this process, which improves the strength and ductility of the weld. Also, this process is more efficient in terms of energy consumption and environmental compatibility than fusion welding processes. In addition, due to the reduction of residual stresses (due to the reduction of heat flux), the distortion of finished products is reduced [4, 5]. The FSW was first developed for the welding of aluminum alloys and subsequently applied to various materials and alloys. This process is used in many industries such as aerospace, automotive, railways, shipbuilding and marine structures [6–8].

✉ Mahdi Vahdati
vahdati@shahroodut.ac.ir

[1] Faculty of Mechanical and Mechatronics Engineering, Shahrood University of Technology, Shahrood, Iran

[2] Department of Mechanical Engineering, Malayer University, Malayer, Iran

[3] Department of Engineering, Mahabad Branch, Islamic Azad University, Mahabad, Iran

[4] Department of Mechanical Engineering, University of Zakho, Zakho, Kurdistan Region, Iraq

In FSW process, a non-consumable rotating tool, including pin and shoulder, penetrates into the material and applies the vertical force to the workpiece. The friction between the workpiece and the tool increases the temperature in the welding zone. Thus, the material softens around the pin, and as a result, the workpiece will undergo plastic deformation. The linear movement of the tool moves the material from the advancing side to the retreating side. Then, the material in the back of the pin is blended and stabled by the tool shoulder, resulting in a solid joint [9–11]. The principles of the FSW are schematically illustrated in Fig. 1.

The FSW causes the creation of fine-grained microstructure in the stir zone, because the dynamic recrystallization occurs by severe plastic deformation [12, 13]. Therefore, the improved mechanical properties are observed in the workpiece. Although the input heat in the FSW is lower than the fusion welding, nevertheless, the softening phenomenon is generally observed in the friction stir welding of heat-treatable aluminum alloys. The dissolution or coarsening of the reinforcing precipitates causes the occurrence of softening, which leads to the decreased mechanical properties of the joints [14–16]. In order to overcome this challenge, the cooling rate can be increased and the mechanical properties of the joint can be improved by reducing the maximum temperature. For this purpose, external cooling has been used in several types of solid-state welding processes [17–19].

The submerged friction stir welding (SFSW) has been introduced as an improved method of the FSW in which water is used as the cooling fluid and plays an important role in adjusting the temperature gradient of the weld joint [20–22]. In this process, welding is done underwater. Therefore, the process is carried out in a water tank or in a condition where water continuously passes through the surface of the workpiece. During the SFSW, the high heat absorption capacity of the water reduces the heat transfer rate to the thermo-mechanically affected zone (TMAZ) and the heat-affected zone (HAZ). Therefore, the low temperatures in these zones cannot lead to precipitate coarsening [23]. It also decreases the width of the HAZ and TMAZ zones due to the reduced heat input [23, 24]. The SFSW improves the mechanical properties by reducing various defects of welding such as porosity, volume shrinkage, solidification cracking and distortion due to residual stresses. The SFSW process is appropriate for heat-sensitive alloys within the welding process. Therefore, it is widely used for aluminum alloys [25, 26].

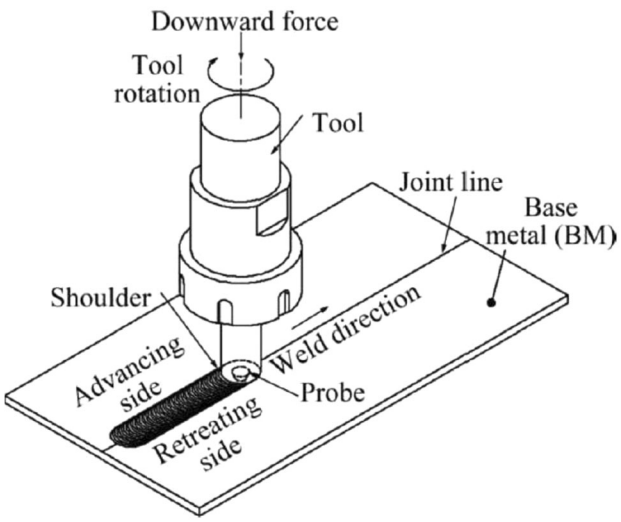

Fig. 1 Principles of FSW operation [9]

Due to the severe plastic deformation of the material in the FSW and SFSW, various microstructural transformations occur at the different areas of the joint cross section. These microstructural transformations lead to changes in the mechanical properties of the joint. The tensile behavior of the joint in FSW and SFSW is considerably affected by stirring, heating, and cooling conditions [27–30]. The type of cooling (air or water) plays an important role to improve the tensile properties of the joint [26, 27]. Researchers' findings have illustrated that the tensile properties of SFSW joint are better than the FSW joint [23, 25].

Liu et al. [26] investigated the tensile properties of AA2219 based on the use of air and water as coolants. The results showed the increased tensile strength of the joint in the SFSW due to the grains refinement and increase of dislocation density. Also, Wang et al. [31] obtained similar results in the SFSW of AA7055. The results showed that the tensile strength of the joint in the water environment increased by 15% compared to the air, which was due to the improvement of the thermal cycle and its effect on the solid solution strengthening. Kishta and Darras [32] investigated the tensile properties of the non-heat-treatable AA5083 in the air and water cooling environments. The results showed the increased tensile strength of the joint in the SFSW and approached to the strength of the base metal.

On the other hand, variations in the tool rotational speed [29, 32], welding speed [28, 33], and depth of tool penetration also lead to changes in the frictional and stirring conditions, thus affecting the tensile strength of the joint. The SFSW of AA2219 shows that the increase of the tool rotational speed to a certain level improves the tensile strength of the joint due to the increase of strain-hardening effect [23]. Also, with increasing the welding speed, the tensile strength increases, which is due to the sufficient heating and material stirring [28, 33]. The tensile strength is less influenced by the changes in depth of tool penetration [29]. Increasing the depth of tool penetration results in

increased forging operation and greater mixing of the material, which causes increased tensile strength.

A review of the FSW and SFSW research shows that the different variables influence the tensile strength of the joint and in most studies, and the effects of each parameter are independently investigated. Therefore, considering the advantages of FSW and SFSW in joining of aluminum heat-treatable alloys, in this study, statistical analysis, mathematical modeling, and optimization of parameters affecting the yield strength and tensile strength of Al7075-T6 butt joint was investigated for both processes. For this purpose, the response surface methodology was selected as the design of experiment method. Then, the statistical analysis of the parameters affecting the yield strength and tensile strength of the joints was studied. The accuracy and precision of regression equations were evaluated using the results of the ANOVA and regression analysis of experimental data. Also, the effect of input variables such as tool rotational speed, tool feed rate, tool tilt angle and tool shoulder diameter on the yield strength and ultimate tensile strength (UTS) of the joints was studied. According to the review of FSW and SFSW, the most important innovation of the present paper compared with the published research is as follows: type of output parameters of the process, type of input variables of the process, the method of experiment design and statistical analysis (RSM), extracting the regression equations of response parameters (yield strength and ultimate tensile strength) and optimization of input variables affecting the response parameters using the desirability function.

2 Statistical Analysis and Optimization of the FSW Process

Two important factors of yield stress and ultimate tensile strength are used to evaluate the yield strength and tensile strength of the produced joints in the FSW and SFSW processes. The values of these two parameters are obtained through the tensile test. Therefore, in the present study, the yield strength and ultimate tensile strength of the joint were selected as the response variables.

It should be noted that the applied force in FSW process induced by welding input parameters, including tool geometry, workpiece material and process parameters, play a key role in this process. For a given set of tool and material characteristics, changes in process parameters result in variation of applied force. Pei and Dong [34] calculated the applied force to the tool axis (F_z) in the FSW process from the following equation:

$$F_z = \pi\left(R^2 - r^2\right)P \tag{1}$$

In this equation, R is the shoulder radius, r is the pin radius, and P is the applied pressure by the tool shoulder on the workpiece surface. The presented equation by Chen and Kovacevic [35] can be used to calculate the axial pressure (P). They predicted the heat generated (Q) in the "tool-workpiece" interface by the following equation:

$$Q = \frac{2\pi\omega\mu P(R^3 - r^3)}{3} \tag{2}$$

In this equation, ω is the angular velocity of the tool, μ is the friction coefficient, P is the axial pressure, R is the shoulder radius and r is the pin radius.

Based on the review research of the FSW, four variables, including tool rotational speed, tool feed rate, tool shoulder diameter, and tool tilt angle (deviation angle relative to the vertical axis), were selected as the experimental input variables, and each of them was investigated at five levels. The range of changes in each of these factors was determined based on the initial experiments that were successful (Table 1).

Table 2 shows the parameters that have not been considered as variable during the FSW and SFSW processes.

It should be noted that the input variables of the SFSW and their levels will be extracted and determined after the statistical analysis and optimization of the FSW process.

2.1 Experimental Set-Up

In the current study, the response surface methodology has been used as the design of experiments method [36–38]. In most problems related to the RSM, the relationship between the responses and the input variables is unknown. So the target is to find an appropriate approximation of the relationship between the response variable (y) and the set of independent input variables (x). In this research, the approximation function as a second-order model has been used, which is written as follows:

$$y = \beta_0 + \sum_{i=1}^{k} \beta_i x_i + \sum_{i=1}^{k} \beta_{ii} x_i^2 + \sum_{i} \sum_{j} \beta_{ij} x_i x_j + \varepsilon \tag{3}$$

In the above equation, β_0 is the constant value, β_i is the linear coefficient, β_{ii} is the quadratic coefficient, β_{ij} is the interaction coefficient, k is the number of independent variables, and ε is the error value of the response.

The Design Expert software [39] has been used to design experiments and statistical analysis. Table 3 shows the design of the FSW experiments. As shown in Table 3, seven experiments were repeated at the central levels of the parameters.

Table 1 Input variables and their range of changes in the FSW

Variable	Symbol	Unit	− 2	− 1	0	+ 1	+ 2
Tool rotational speed	*N*	rpm	400	600	800	1000	1200
Tool feed rate	*S*	mm/min	20	40	60	80	100
Tool shoulder diameter	*D*	mm	9	12	15	18	21
Tool tilt angle	*A*	Degree	0	1.5	3	4.5	6

Table 2 Fixed parameters in FSW and SFSW processes

Parameter	Description or set value
Workpiece material	Al7075-T6 alloy
Workpiece thickness	10 mm
Tool material	H13 tool steel
Pin geometry	Grooved conical
Depth of pin penetration	4 mm
Number of passes	1 pass
Direction of tool rotation	Clockwise
Length of welding path	90 mm
Joint type	Butt joint

The material of the experiment was the Al7075-T6. Table 4 shows the chemical composition of the alloy.

The Al7075-T6 plates were subjected to aging treatment in accordance with the AMSH6088 [41]. For this purpose, the dissolution process was first done on the samples for 1 h at 480 °C. Then, the alloy plates were subjected to quenching to obtain a super-saturated solid solution. Subsequently, the artificial aging was done on the samples for 24 h at 120 °C. Finally, the alloy plates were cooled in air.

The FSW tools were made of H13 tool steel in five shoulder diameters of 9, 12, 15, 18 and 21 mm and with a grooved conical geometry in the pin. The shoulder and pin diameters were indicated by "*a*" and "*d*", respectively, in Fig. 2.

Figure 3 shows the placement of the parts in the form of butt joint in the fixture. Then, the FSW tests were done according to the 31 parameter combinations listed in Table 3 using the FP4MK universal milling machine (Fig. 4). Figure 5 shows a sample of the produced butt joint.

The tensile test has been used to measure the yield strength and ultimate tensile strength of the welded joints. For this purpose, the tensile specimens were produced according to the ASTM E8. The samples were extracted perpendicular to the FSW path using wire-EDM machine. Then, each sample was tested at the room temperature using an INSTRON tensile machine at a feed rate of 2 mm/min. Figure 6 shows some of samples which fractured after the tensile test.

The measurement results of the yield strength and ultimate tensile strength of the FSW joints are presented in Table 3.

2.2 Results Analysis

Data analysis was performed using analysis of variance (ANOVA). Regression analysis was also used to create the mathematical equations between the response variables and input parameters [42]. The confidence level (α) was equal to 0.05. Tables 5 and 6 show the results of the ANOVA of the regression model for the yield strength and ultimate tensile strength of the produced joints in the FSW, respectively.

The effectiveness of a term is determined by its *P* value. The smaller *P* value of a term is related to its more meaningful value in the model. Therefore, with $\alpha = 0.05$ and based on the ANOVA results, the first-order parameter *N* (tool rotational speed), the interactional term *N.D* (tool rotational speed multiplied by the tool shoulder diameter) and the second-order term N^2 (squared of the tool rotational speed) are the most important terms affecting the yield strength of the joints. The first-order parameter *N* (tool rotational speed) and the second-order term N^2 (squared of the tool rotational speed) have been identified as the most important terms affecting the ultimate tensile strength of the joints.

The "lack of fit" test is used to validate the regression model. By confirming the non-meaningful of the "lack of fit" test ($P_{\text{Lack of fit}} > 0.05$), it can be concluded that the model can fit well to the data. As shown in Tables 5 and 6, the "lack of fit" test for the response variables is not meaningful, and thus the presented model shows the data trend correctly. On the other hand, the best analysis is done when regression term is significant, and the "lack of fit" term is insignificant simultaneously [42]. Therefore, regarding the *P* values (Tables 5, 6), it can be seen that the regression term is significant, and the "lack of fit" term is insignificant. Hence, the ability of the fitted model to predict the changes of response variables as a function of input variables is confirmed.

The residual is defined as the difference between the response in the experimental test and the predicted

Table 3 Design of FSW experiments and measurement results

Test no.	Input variables				Response variables	
	Rotational speed (*N*)	Feed rate (*S*)	Shoulder diameter (*D*)	Tilt angle (*A*)	Tensile strength (MPa)	Ultimate tensile strength (MPa)
1	0	0	0	2	298	350
2	2	0	0	0	392	430
3	0	0	0	0	385	435
4	1	− 1	1	− 1	370	398
5	0	0	0	0	385	435
6	0	0	0	0	385	435
7	0	2	0	0	390	432
8	0	0	0	0	385	435
9	1	− 1	− 1	1	302	355
10	1	− 1	1	1	370	390
11	− 1	1	− 1	− 1	285	331
12	− 1	− 1	− 1	1	270	308
13	1	1	− 1	− 1	298	362
14	− 1	− 1	1	1	252	317
15	0	0	− 2	0	310	370
16	− 1	1	1	− 1	275	320
17	− 1	1	1	1	267	313
18	1	− 1	− 1	− 1	288	347
19	− 1	− 1	1	− 1	290	345
20	0	0	0	0	385	435
21	1	1	1	− 1	372	415
22	− 2	0	0	0	255	315
23	0	0	2	0	391	445
24	0	0	0	0	385	435
25	− 1	1	− 1	1	270	312
26	0	0	0	− 2	364	430
27	0	0	0	0	385	435
28	1	1	1	1	308	377
29	− 1	− 1	− 1	− 1	261	320
30	1	1	− 1	1	265	322
31	0	− 2	0	0	314	365

Table 4 Chemical composition of Al7075-T6 [40]

Element	Weight percent (%)
Al	87.1–91.4
Zn	5.1–6.1
Mg	2.1–2.9
Cu	1.2–2
Fe	0.5
Si	0.4
Mn	0.3
Cr	0.18–0.28
Ti	0.2

response by the regression model. The normal probability graph has been used to evaluate the accuracy of the normal distribution of the residuals. As shown in Fig. 7, generally, the residuals in both graphs follow a straight line, and there is no evidence that they are abnormal and asymmetrical.

2.2.1 Yield Strength

The following relationship presents the regression equation of the yield strength as a function of the coded input variables:

Fig. 2 Design and manufacture a sample of FSW tool

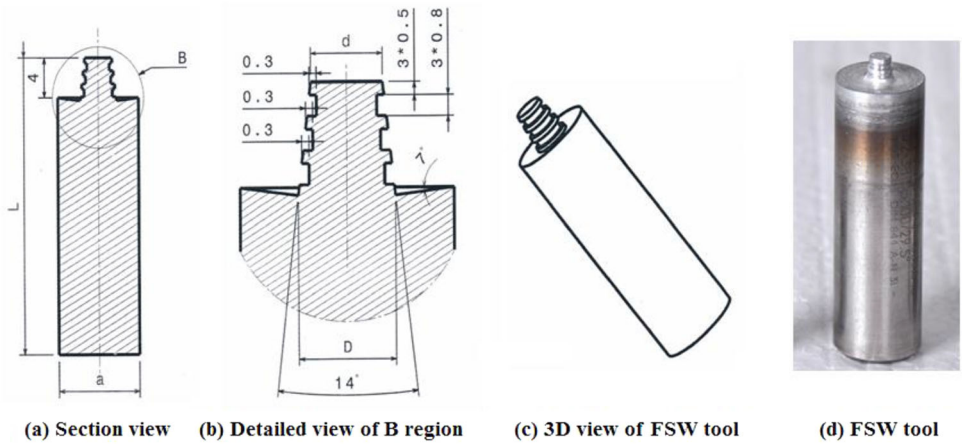

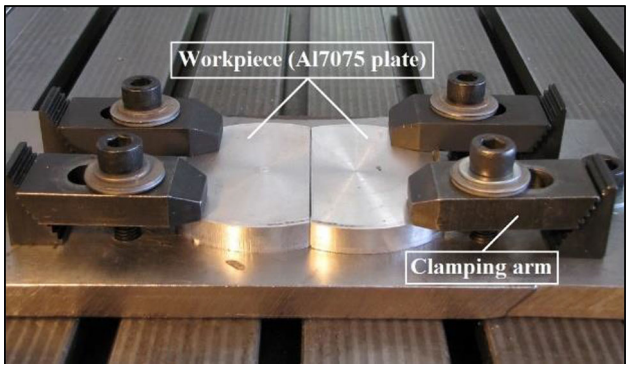

Fig. 3 Arrangement of the parts in the fixture

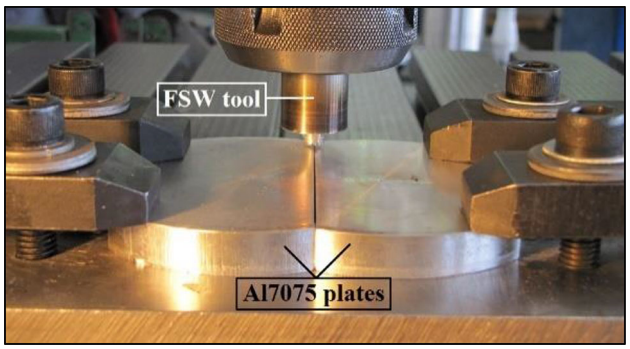

Fig. 4 Execution of the FSW process

$$(\text{Yield Stress})^{-0.14} = 0.43 - 0.011N - 1.292 \times 10^{-3}S - 6.621 \times 10^{-3}D + 4.431 \times 10^{-3}A - 0.013ND + 0.018N^2 + 0.011S^2 + 0.012D^2 + 0.015A^2 \quad (4)$$

Regarding the calculation of the regression equation, the yield strength of the joints can be predicted in terms of the input variables before the FSW execution. As can be seen in Eq. (4), the linear effect of input variables on the yield strength according to their importance are as follows: tool rotational speed, tool shoulder diameter, tool tilt angle and tool feed rate. Also, the quadratic effect of input variables according to their importance are as follows: tool rotational speed, tool tilt angle, tool shoulder diameter and tool feed rate.

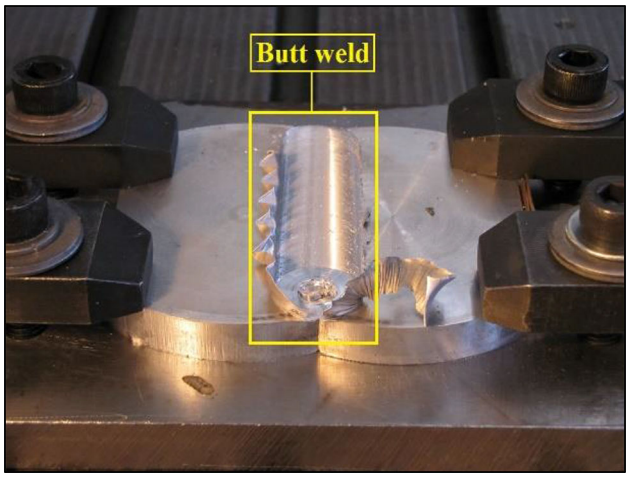

Fig. 5 A sample of butt joint in the FSW

On the other hand, the changes of response variable according to the input variables can be represented as the 3D surface plots. As can be seen in Fig. 8a, adjusting the values of tool rotational speed and tool shoulder diameter in the range of maximum level results in the maximum yield strength. Therefore, if a tool with a shoulder diameter of 21 mm is used, and rotational speed increases from 400 to 1200 rpm, will increases the yield strength. In this situation, an increase of the tool rotational speed increases the frictional heat. On the other hand, the created frictional heat by increasing the contact surface of the tool and the workpiece (increasing the tool shoulder diameter) results in more efficient mixing of the material in the joint seam, which results in an increase in the yield strength.

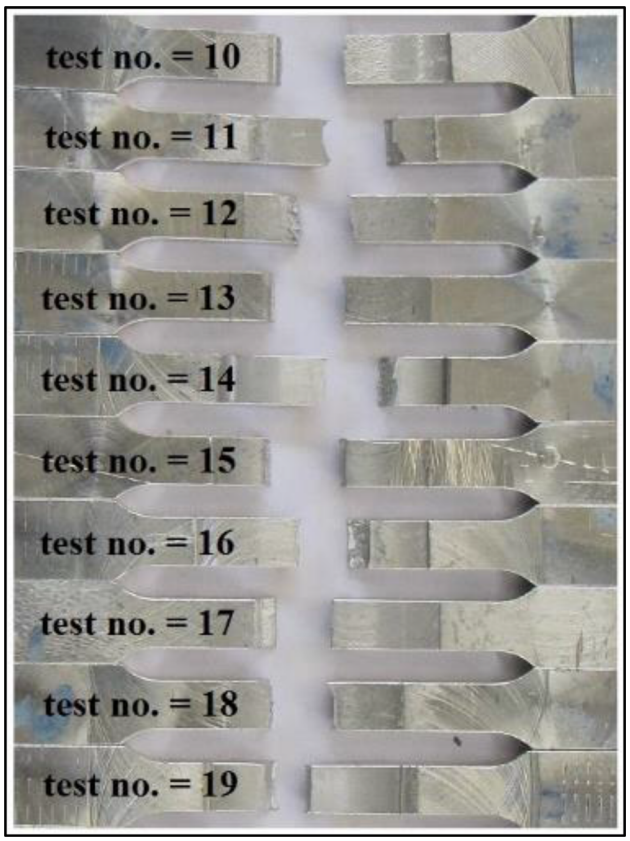

Fig. 6 A number of fractured joints (FSW)

2.2.2 *Ultimate Tensile Strength*

The following relationship presents the regression equation of the ultimate tensile strength as a function of the coded input variables:

$$\begin{aligned}(\mathrm{UTS})^{-0.3} = {} & 0.16 - 7.563 \times 10^{-3}N - 1.007 \times 10^{-3}S \\ & - 4.078 \times 10^{-3}D + 3.517 \times 10^{-3}A + 0.013N^2 \\ & + 8.71 \times 10^{-3}S^2 + 7.646 \times 10^{-3}D^2 + 9.902 \\ & \times 10^{-3}A^2 \end{aligned} \quad (5)$$

Regarding the calculation of the regression equation, it is possible to select the appropriate combination of input variables to achieve the maximum ultimate tensile strength. As can be seen in Eq. (5), the linear effect of input variables on the ultimate tensile strength according to their importance, are as follows: tool rotational speed, tool shoulder diameter, tool tilt angle and tool feed rate.

As shown in Fig. 8b, adjusting the values of tool feed rate and tool tilt angle in the range of central level results in the maximum ultimate tensile strength. Also, by adjusting the tool tilt angle to a specified value, decreasing the tool feed rate reduces the ultimate tensile strength due to the increased heat input to the joint seam. On the other hand, increasing the tool feed rate leads to lower heating and undesirable stirring of the material, which leads to a decrease in the ultimate tensile strength and the make of microstructural defects.

2.3 Optimization and Verification

In this study, the desirability method is used as an optimization technique [42]. The purpose of the desirability function is to maximize the response variables (yield strength and ultimate tensile strength). Therefore, the desirability function is defined as follows:

Table 5 ANOVA of the regression model for the yield strength of FSW joints

Source of variation	Sum of squares	Degrees of freedom	Mean square	*F* value	*P* value
Model	2.453E − 003	9	2.726E − 004	9.33	< 0.0001
N (rotational speed)	7.709E − 004	1	7.709E − 004	26.39	< 0.0001
S (feed rate)	1.002E − 005	1	1.002E − 005	0.34	0.5643
D (shoulder diameter)	2.631E − 004	1	2.631E − 004	9.01	0.0068
A (tilt angle)	1.178E − 004	1	1.178E − 004	4.03	0.0576
N.D	1.704E − 004	1	1.704E − 004	5.83	0.0249
N^2	5.689E − 004	1	5.689E − 004	19.47	0.0002
S^2	2.317E − 004	1	2.317E − 004	7.93	0.0103
D^2	2.451E − 004	1	2.451E − 004	8.39	0.0086
A^2	4.093E − 004	1	4.093E − 004	14.01	0.0012
Residual	6.134E − 004	21	2.921E − 005	–	–
Lack of fit	6.134E − 004	15	4.089E − 005	0.67	0.4531
Pure error	0	6	0	–	–
Total	3.067E − 003	30	–	–	–

Table 6 ANOVA of the regression model for the ultimate tensile strength of FSW joints

Source of variation	Sum of squares	Degrees of freedom	Mean square	*F* value	*P* value
Model	1.065E − 003	8	1.331E − 004	9.46	< 0.0001
N (rotational speed)	3.432E − 004	1	3.432E − 004	24.40	< 0.0001
S (feed rate)	6.087E − 006	1	6.087E − 006	0.43	0.5175
D (shoulder diameter)	9.977E − 005	1	9.977E − 005	7.09	0.0142
A (tilt angle)	7.423E − 005	1	7.423E − 005	5.28	0.0315
N^2	2.870E − 004	1	2.870E − 004	20.40	0.0002
S^2	1.356E − 004	1	1.356E − 004	9.64	0.0052
D^2	1.045E − 004	1	1.045E − 004	7.43	0.0123
A^2	1.752E − 004	1	1.752E − 004	12.46	0.0019
Residual	3.094E − 004	22	1.406E − 005	–	–
Lack of fit	3.094E − 004	16	1.934E − 005	0.54	0.3752
Pure error	0	6	0	–	–
Total	1.374E − 003	30	–	–	–

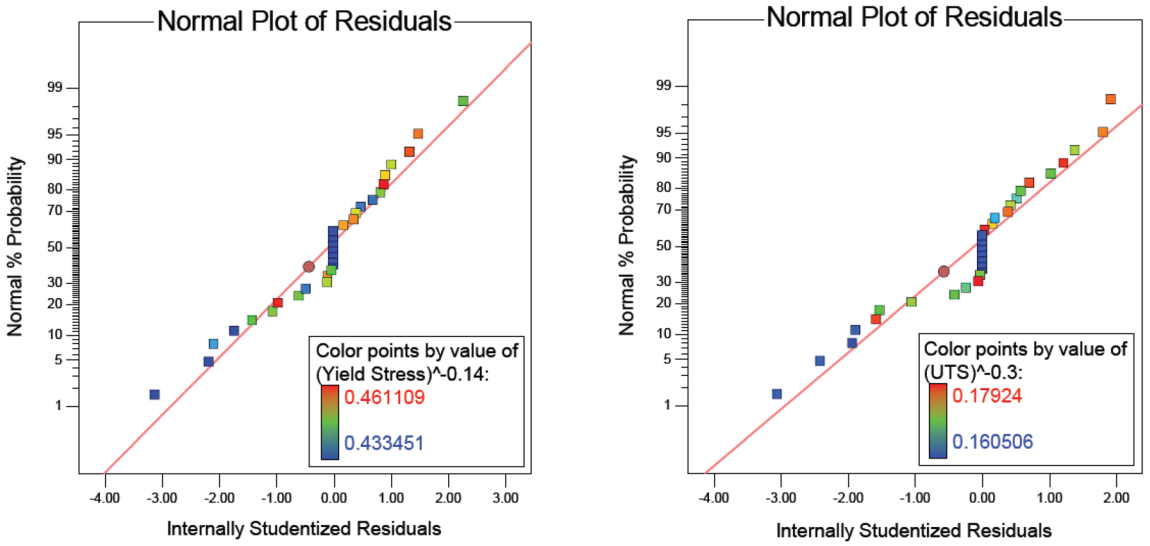

(**a**) Yield strength (**b**) Ultimate tensile strength

Fig. 7 Normal probability diagram

$$d = \begin{cases} 0 & y < L \\ \left(\dfrac{y-L}{U-L}\right)^{r} & L \le y \le U \\ 1 & y > U \end{cases} \quad (6)$$

In the above equation, the parameters L and U are the lower and upper limits of the response value of y, respectively. The form of the desirability function depends on the weight field (r) that is used to describe the degree of importance of the target values. In this study, the weight value is equal to one (1), and the desirability function will be defined in a linear mode. Table 7 shows the optimal combination of input variables with the highest desirability value (0.976) to achieve the maximum values of yield strength and ultimate tensile strength.

Therefore, given the high value of the desirability function, it can be concluded that the optimization process has successfully achieved the desired target. To verify the optimum input parameters, the experimental test is performed by a tool shoulder diameter of 18 mm, and with adjusting the tool rotational speed, tool feed rate and tool tilt angle in the range of optimum values. The small difference between the optimization results and the experimental test confirms the accuracy and precision of the

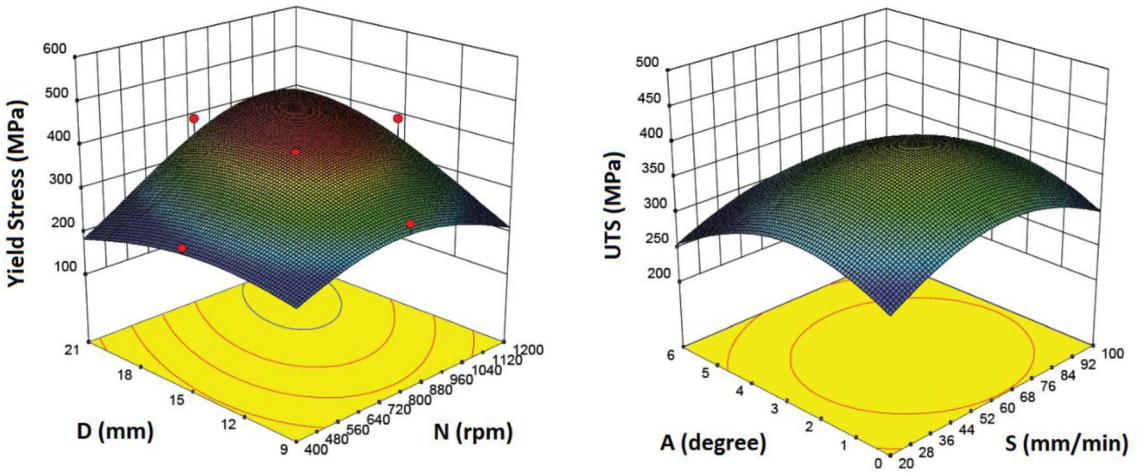

(**a**) Yield strength (The effect of N and D) (**b**) Ultimate tensile strength (The effect of S and A)

Fig. 8 Influence of input variables on the yield strength and ultimate tensile strength of FSW joints

optimization process to determine the optimal combination of input variables (Table 8).

3 Statistical Analysis and Optimization of the SFSW Process

Since the tool rotational speed (*N*) and tool shoulder diameter (*D*) have been identified as the most important linear terms affecting the yield strength and ultimate tensile strength of the FSW joints (Tables 5, 6), and also since the optimum values of the input variables of the FSW are calculated and verified, two variables of tool rotational speed (*N*) and tool shoulder diameter (*D*) have been selected as the input variables of the SFSW, and each of them has been investigated at three levels (Table 9). Also, the values of the tool feed rate (*S*) and tool tilt angle (*A*) are fixed at the optimum values obtained from the FSW process.

3.1 Experimental Set-Up

Table 10 shows the design of ten SFSW experiments, in which two experiments will be repeated at the central levels of the parameters.

Figure 9 shows the placement of the plates in the fixture. As can be seen, the fixture and the workpieces are submerged in a water tank. According to Fig. 10, the value of water depth in which the tool and workpiece are submerged is equal to 55 mm.

The SFSW experiments have been performed according to the 10 parameter combinations listed in Table 10 using the FP4MK universal milling machine (Fig. 10). Figure 11 shows an example of the produced butt joint by the SFSW.

Similar to the FSW, the tensile test is used to measure the response variables. Figure 12 shows the broken joints after the tensile test. The measurement results of the yield strength and ultimate tensile strength of the SFSW joints are presented in Table 10.

Table 7 Optimal values of FSW input variables

Variable type	Variable name	Unit	Optimal value
Input	Tool rotational speed	rpm	971.47
	Tool feed rate	mm/min	62.59
	Tool shoulder diameter	mm	18.14
	Tool tilt angle	Degree	2.05
Response	Yield strength	MPa	415.963
	Ultimate tensile strength	MPa	445.001

Table 8 The results obtained from optimization and verification test

Response variable (MPa)	Optimization	Verification test	Difference percent (%)
Yield strength	415.963	392	5.76
Ultimate tensile strength	445.001	420	5.62

3.2 Results Analysis

Tables 11 and 12 show the results of the ANOVA of the regression model for the yield strength and ultimate tensile strength of the produced joints in the SFSW, respectively.

Given $\alpha = 0.05$ and based on the results of the ANOVA, the first-order parameter N (tool rotational speed) and the second-order term D^2 (square of the tool shoulder diameter) are the most important terms affecting the yield strength of the joints as well as the second-order term N^2 (square of the tool rotational speed) is the most important term affecting the ultimate tensile strength of the joints.

As can be seen in Tables 11 and 12, the "lack of fit" test for the response variables is not meaningful, and thus the presented model clearly shows the data trend. On the other hand, it is found that the regression term is significant, and the "lack of fit" term is insignificant. Therefore, the ability of the fitted model to describe and predict the changes of response variables as a function of input variables is confirmed.

The following relationship presents the regression equation of the yield strength as a function of the coded input variables:

$$\begin{aligned}(\text{Yield Stress})^3 &= 3.243 \times 10^7 + 6.098 \times 10^6 N \\ &\quad - 7.774 \times 10^5 D - 2.005 \times 10^6 ND \\ &\quad + 1.535 \times 10^7 N^2 + 2.618 \times 10^7 D^2\end{aligned} \tag{7}$$

As can be seen in Eq. (7), the linear effect of input variables on the yield strength according to their importance are as follows: tool rotational speed and tool shoulder diameter. Also, the quadratic effect of input variables according to their importance are as follows: tool shoulder diameter and tool rotational speed. As shown in Fig. 13a, with increasing or decreasing the values of tool rotational speed and tool shoulder diameter relative to the central level (1000 rpm and 18 mm), the yield strength of the joints increases. It should be noted that an excessive increase in the tool rotational speed or tool shoulder diameter results in increased heat input to the joint and decrease its strength.

The following relationship presents the regression equation of the ultimate tensile strength as a function of the coded input variables:

$$\begin{aligned}(\text{UTS})^{-3} &= 1.745 \times 10^{-8} - 6.814 \times 10^{-10} N \\ &\quad + 8.393 \times 10^{-11} D + 3.371 \times 10^{-10} ND \\ &\quad - 3.999 \times 10^{-9} N^2 - 3.416 \times 10^{-9} D^2\end{aligned} \tag{8}$$

As can be seen in Eq. (8), the linear effect of input variables on the ultimate tensile strength according to their importance are as follows: tool rotational speed and tool shoulder diameter. Also, the quadratic effect of input variables according to their importance are as follows: tool rotational speed and tool shoulder diameter. As shown in Fig. 13b, similar to the yield strength trend, by increasing or decreasing the values of the tool rotational speed and tool shoulder diameter relative to the central level (1000 rpm and 18 mm), the ultimate tensile strength of the joint increases. It should be noted that excessive reduction of tool rotational speed results in a reduction of the stirring effect of the tool, which results in a reduction of the tensile strength.

3.3 Optimization and Verification

Table 13 shows the optimal combination of input variables with the highest desirability value (equal to 1) to achieve the maximum values of yield strength and ultimate tensile strength.

To verify the optimum combination, the experimental test is performed by a tool shoulder diameter of 15 mm at a rotational speed of 1200 rpm and adjusting the feed rate and tilt angle, near the optimum values obtained by the

Table 9 Input variables and their range of changes in the SFSW

Variable	Symbol	Unit	− 1	0	+ 1
Tool rotational speed	N	rpm	800	1000	1200
Tool shoulder diameter	D	mm	15	18	21

Table 10 Design of SFSW experiments and measurement results

Test no.	Input variables		Response variables	
	Rotational speed (*N*)	Shoulder diameter (*D*)	Tensile strength (MPa)	Ultimate tensile strength (MPa)
1	1000	15	389	409
2	1000	18	321	392
3	800	15	412	461
4	800	21	417	472
5	800	18	327	398
6	1000	21	385	404
7	1000	18	321	392
8	1200	21	421	469
9	1200	15	431	480
10	1200	18	390	428

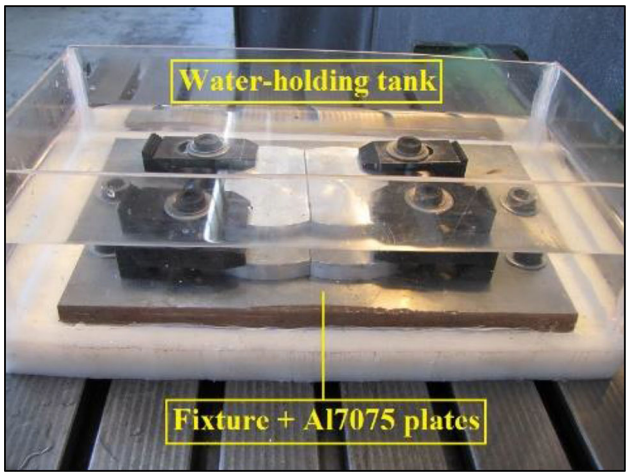

Fig. 9 Arrangement of the fixture and the plates in the water tank

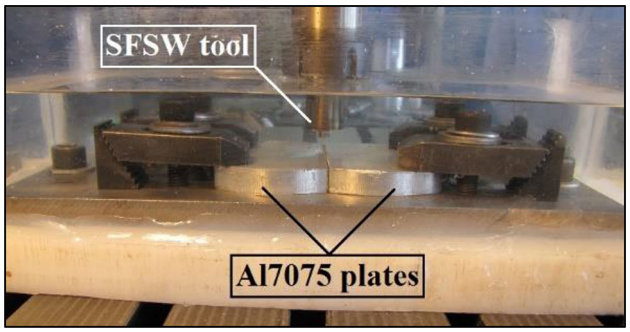

Fig. 10 Execution of the SFSW process

FSW process. The small difference between the optimization results and the experimental test confirms the accuracy and precision of the optimization process to determine the optimal combination of input variables (Table 14).

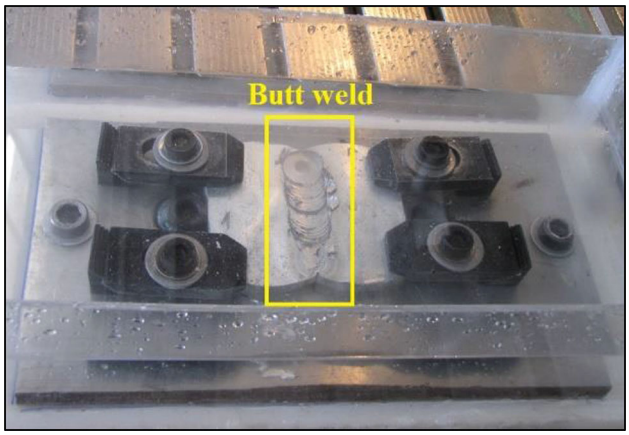

Fig. 11 A sample of butt joint in the SFSW

4 Conclusion

In this paper, statistical analysis and optimization of the yield strength and tensile strength of Al7075 butt joint produced by FSW and SFSW were performed using response surface methodology and desirability approach. The important results of this study are summarized as follows:

- ANOVA results in the FSW process show that the first-order parameter *N* (tool rotational speed), the interactional term *N.D* (tool rotational speed multiplied by the tool shoulder diameter) and the second-order term N^2 (squared of the tool rotational speed) are the most important terms affecting the yield strength of the joints. Also, the first-order parameter *N* (tool rotational speed) and the second-order term N^2 (squared of the tool rotational speed) have been identified as the most important terms affecting the ultimate tensile strength of the FSW joints.

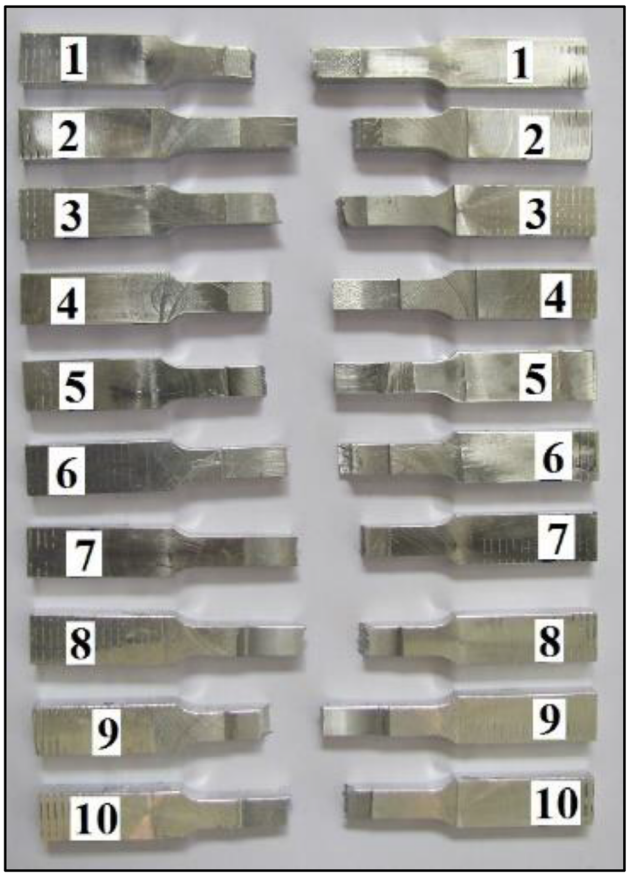

Fig. 12 The fractured joints in the tensile test (SFSW)

- Based on the ANOVA results in the SFSW process, the first-order parameter N (tool rotational speed) and the second-order term D^2 (squared of the tool shoulder diameter) are the most important terms affecting the yield strength of the joints. Also, the second-order term N^2 (squared of the tool rotational speed) is the most important term affecting the ultimate tensile strength of the SFSW joints.
- The competency and adequacy of regression models related to the yield strength and ultimate tensile strength in both FSW and SFSW have been evaluated by a "lack of fit" test and normal probability graph. The ability of the fitted models to describe and predict the changes of response variables is confirmed.
- The regression equations have been calculated to predict the values of yield strength and ultimate tensile strength of the produced joints in both FSW and SFSW as a function of the linear, interactional and quadratic effects of input variables. Therefore, it is possible to select the appropriate combination of input variables to achieve the maximum response variables.
- The regression equation of yield strength and ultimate tensile strength in the FSW process shows that the linear effect of input variables on the response variables according to their importance is as follows: tool rotational speed, tool shoulder diameter, tool tilt angle and tool feed rate.
- The regression equation of yield strength and ultimate tensile strength in the SFSW process shows that the linear effect of input variables on the response parameters according to their importance is as following: tool rotational speed and tool shoulder diameter.
- The surface plots in the FSW process show that adjusting the values of tool shoulder diameter and tool rotational speed close to the maximum level results in the maximum yield strength of the joint. Also, adjusting the values of feed rate and tilt angle of the tool close to the central level result in the maximum ultimate tensile strength of the joint.
- The optimal values of the FSW and SFSW input variables have been calculated to obtain the maximum yield strength and ultimate tensile strength. The desirability values are 0.976 and 1 for FSW and SFSW processes, respectively. Therefore, the high values of

Table 11 ANOVA of the regression model for the yield strength of SFSW joints

Source of variation	Sum of squares	Degrees of freedom	Mean square	F value	P value
Model	2.774E + 015	5	5.549E + 014	19.51	0.0065
N (rotational speed)	2.231E + 014	1	2.231E + 014	7.84	0.0488
D (shoulder diameter)	3.626E + 012	1	3.626E + 012	0.13	0.7391
$N.D$	1.609E + 013	1	1.609E + 013	0.57	0.4939
N^2	5.499E + 014	1	5.499E + 014	19.33	0.0117
D^2	1.599E + 015	1	1.599E + 015	56.20	0.0017
Residual	1.138E + 014	4	2.845E + 013	–	–
Lack of fit	1.138E + 014	3	3.793E + 013	0.26	0.4685
Pure error	0	1	0	–	–
Total	2.888E + 015	9	–	–	–

Table 12 ANOVA of the regression model for the ultimate tensile strength of SFSW joints

Source of variation	Sum of squares	Degrees of freedom	Mean square	*F* value	*P* value
Model	8.059E − 017	5	1.612E − 017	8.62	0.0289
N (rotational speed)	2.786E − 018	1	2.786E − 018	1.49	0.2893
D (shoulder diameter)	4.226E − 020	1	4.226E − 020	0.023	0.8878
N.D	4.545E − 019	1	4.545E − 019	0.24	0.6479
N^2	3.731E − 017	1	3.731E − 017	19.95	0.0111
D^2	2.723E − 017	1	2.723E − 017	14.56	0.0189
Residual	7.481E − 018	4	1.870E − 018	–	–
Lack of fit	7.481E − 018	3	2.494E − 018	0.33	0.7938
Pure error	0	1	0	–	–
Total	8.807E − 017	9	–	–	–

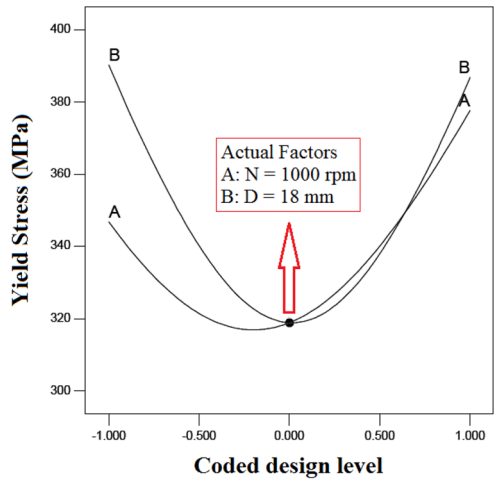

(**a**) Yield strength (The effect of N and D)

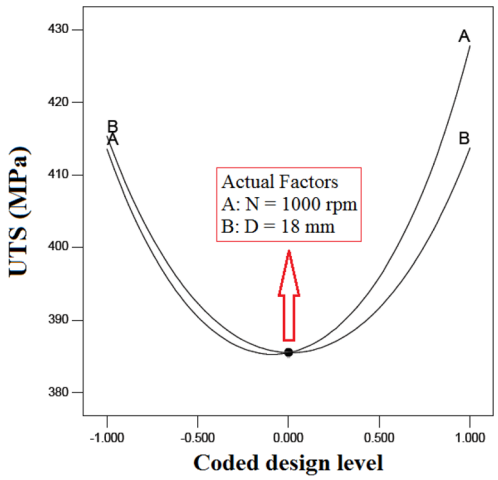

(**b**) Ultimate tensile strength (The effect of N and D)

Fig. 13 Effect of input variables on the yield strength and ultimate tensile strength of SFSW joints

Table 13 Optimal values of SFSW input variables

Variable type	Variable name	Unit	Optimal value
Input	Tool rotational speed	rpm	1200
	Tool shoulder diameter	mm	15
Response	Yield strength	MPa	435.929
	Ultimate tensile strength	MPa	481.875

Table 14 The results obtained from optimization and verification test

Response variable (MPa)	Optimization	Verification test	Difference percent (%)
Yield strength	435.929	431	1.13
Ultimate tensile strength	481.875	480	0.39

desirability function indicate that the optimization process has successfully achieved the research targets.

- The small differences between the optimization results and the verification experiments (less than 6% for the FSW and less than 2% for the SFSW) confirm the

accuracy and precision of the optimization process to determine the optimal combination of input variables.

References

1. Qin B, Yin F C, Zeng C Z, Xie J C, and Shen J, *Trans Nonferrous Met Soc China* **29** (2019) 1864.
2. Tamasgavabari R, Ebrahimi A R, Abbasi S M, and Yazdipour A R, *J Manuf Process* **49** (2020) 413.
3. Thomas W M, Nicholas E D, Needham J C, Murch M G, Smith P T, and Dawes C J, *Friction Stir Butt Welding*. Int. Patent No. PCT/GB92/02203 (1991).
4. Guerra M, Schmidt C, Mcclure L C, Murr L E, and Nunes A C, *Mater Charact* **49** (2003) 95.
5. Rhodes C G, Mahoney M W, Bingel W H, Spurling R A, and Bampton C C, *Scr Mater* **36** (1997) 69.
6. Zhao J, Jiang F, Jian H G, Wen K, Jiang L, and Chen X B, *Mater Des* **31** (2010) 306.
7. Steel R J, Packer S M, Fleck R D, Sanderson S, and Tucker C, in *Proceedings of the 1st International Joint Symposium on Joining and Welding*, (eds) Fujii H, Woodhead Publishing (2013), p 125.
8. Thomas W M, and Nicholas E D, *Mater Des* **18** (1997) 269.
9. Siddiquee A N, and Pandey S, *Int J Adv Manuf Technol* **73** (2014) 479.
10. Gite R A, Loharkar P K, and Shimpi R, *Mater Today Proc* **19** (2019) 361.
11. Cho J H, Han S H, and Lee C, *Mater Lett* **180** (2016) 157.
12. Woo W, Balogh L, Ungár T, Choo H, and Feng Z, *Mater Sci Eng A* **498** (2008) 308.
13. Jata K V, and Semiatin S L, *Scr Mater* **43** (2000) 743.
14. Liu H J, Fujii H, Maeda M, and Nogi K, *Mater Sci Lett* **22** (2003) 1061.
15. Guo Y, Ma Y, and Wang F, *Theor Appl Fract Mech* **104** (2019) 102372.
16. Cabibbo M, Mcqueen H J, Evangelista E, Spigarelli S, Paola M D, and Falchero A, *Mater Sci Eng A* **460–461** (2007) 86.
17. Fratini L, Buffa G, and Shivpuri R, *Int J Adv Manuf Technol* **43** (2009) 664.
18. Sakurada D, Katoh K, and Tokisue H, *J Jpn Inst Light Met* **52** (2002) 2.
19. Derazkola H A, and Khodabakhshi F, *Int J Adv Manuf Technol* **102** (2019) 4383.
20. Rouzbehani R, Kokabi A H, Sabet H, Paidar M, and Ojo O O, *J Mater Process Technol* **262** (2018) 239.
21. Mofid M A, Abdollah-Zadeh A, Ghaini F M, and Gur C H, *Metall Mater Trans A* **43** (2012) 5106.
22. Sabari S S, Malarvizhi S, Balasubramanian V, and Reddy G M, *Def Technol* **12** (2016) 324.
23. Zhang H J, Liu H J, and Yu L, *Mater Des* **32** (2011) 4402.
24. Nelson T W, Steel R J, and Arbegast W J, *Sci Technol Weld Join* **8** (2003) 283.
25. Xua W F, Liu J H, Chen D L, Luan G H, and Yao J S, *Mater Sci Eng A* **548** (2012) 89.
26. Liu H J, Zhang H J, Huang Y X, and Lei Y, *Trans Nonferrous Met Soc China* **20** (2010) 1387.
27. Wang Q, Zhao Z, Zhao Y, Yan K, and Zhang H, *Mater Des* **88** (2015) 1366.
28. Liu H J, Zhang H J, and Yu L, *Mater Des* **32** (2011) 1548.
29. Zhang H, and Liu H, *Mater Des* **45** (2013) 206.
30. Zhang H J, Liu H J, and Yu L, *J Mater Eng Perform* **21** (2012) 1182.
31. Wang Q, Zhao Y, Yan K, and Lu S, *Mater Des* **68** (2015) 97.
32. Kishta E E, and Darras B, *Proc Inst Mech Eng Part B J Eng Manuf* **230** (2014) 458.
33. Sabari S S, Malarvizhi S, and Balasubramanian V, *J Mater Process Technol* **237** (2016) 286.
34. Pei X, and Dong P, *Int J Adv Manuf Technol* **95** (2018) 3549.
35. Chen C M, and Kovacevic R, *Int J Mach Tools Manuf* **43** (2003) 1319.
36. Myers R H, Montgomery D C, and Anderson-Cook C M, *Response Surface Methodology: Process and Product Optimization Using Designed Experiments*, Wiley, Hoboken (2016), ISBN 978-1-118-91601-8.
37. Vahdati M, and Moradi M, *Iran J Mater Form* **7** (2020) 32.
38. Moradi M, Arabi H, and Shamsborhan M, *Optik* **202** (2020) 163619.
39. Design Expert Software, http://www.statease.com, available in 1 April 2020.
40. Online Materials Information Resource, http://www.matweb.com , available in 1 April 2020.
41. Heat Treatment of Aluminum Alloys, *Aerospace Material Specification*, AMSH6088 (1997).
42. Montgomery D C, *Design and Analysis of Experiments*, Wiley, Hoboken (2017), ISBN 978-1-119-11347-8.